PAPER

On the isotope effect in compressed superconducting H_3S and D_3S

To cite this article: Dale R Harshman and Anthony T Fiory 2017 *Supercond. Sci. Technol.* **30** 045011

IOP Publishing Superconductor Science and Technology
Supercond. Sci. Technol. 30 (2017) 045011 (5pp) https://doi.org/10.1088/1361-6668/aa5f3c

On the isotope effect in compressed superconducting H_3S and D_3S

Dale R Harshman[1] **and Anthony T Fiory**[2]

[1] Department of Physics, The College of William and Mary, Williamsburg, VA 23185, United States of America
[2] Department of Physics, New Jersey Institute of Technology, Newark, NJ 07102, United States of America

E-mail: drh@physikon.net

Received 8 December 2016, revised 5 February 2017
Accepted for publication 8 February 2017
Published 10 March 2017

Abstract

A maximum superconductive transition temperature $T_C = 203.5$ K has recently been reported for a sample of the binary compound tri-hydrogen sulfide (H_3S) prepared at high pressure and with room temperature annealing. Measurements of T_C for H_3S and its deuterium counterpart D_3S have suggested a mass isotope effect exponent α with anomalous enhancements for reduced applied pressures. While widely cited for evidence of phonon-based superconductivity, the measured T_C is shown to exhibit important dependences on the quality and character of the H_3S and D_3S materials under study; examination of resistance versus temperature data shows that variations in T_C and apparent α are strongly correlated with residual resistance ratio, indicative of sensitivity to metallic order. Correlations also extend to the fractional widths of the superconducting transitions. Using resistance data to quantify and compensate for the evident materials differences between H_3S and D_3S samples, a value of $\alpha = 0.043 \pm 0.140$ is obtained. Thus, when corrected for the varying levels of disorder, the experimental upper limit ($\leqslant 0.183$) lies well below α derived in phonon-based theories.

Keywords: tri-hydrogen sulfide, isotope effect, transition temperature

(Some figures may appear in colour only in the online journal)

Introduction

The highest reported superconducting transition temperature is presently found in highly compressed tri-hydrogen sulfide [1] (H_3S, symmetry group $Im\bar{3}m$ [2]), exhibiting a diamagnetism onset $T_C \sim 200$ K at applied hydrostatic pressure $P = 155$ GPa, with comparative data on D_3S showing $T_C \sim 150$ K [1]. Taken at face value, these data suggest a finite H–D-mass isotope effect with exponent $\alpha \sim 0.4$ and a phonon-based origin for the superconductivity [1].

Prior to its discovery, calculations based on strong electron–phonon coupling and Eliashberg theory predicted $T_C \sim 200$ K for H_3S [3]. Post-discovery formalisms, which consider both harmonic and anharmonic effects in the H vibrations, produce similar findings for H_3S, derive $T_C \sim 150$ K for D_3S, and calculate $\alpha = 0.35$ or $0.38 \leqslant \alpha \leqslant 0.42$ [4–7]. Comparisons made with experiment, such as an apparent divergence in α at low P [8], generally presume that the differences between H_3S and D_3S are intrinsic and free from materials effects. As is shown below, however, interpreting the experimental data is most certainly complicated by the evident effects of disorder on T_C, which are comparatively more prevalent in D_3S samples.

Of particular interest to the present study are data for samples of H_3S and D_3S annealed at temperature T at or above room temperature and $P \gtrsim 150$ GPa; this process is found to reduce the normal-state resistance, while increasing T_C [1, 2]. In H_3S, thermal annealing induces a kinetically controlled phase transformation, as deduced from observations of sharp increases of $T_C \gtrsim 70$ K for $P \gtrsim 160$ GPa [1]. However, such annealing evidently does not completely remove the influence of materials disorder in the samples. The highest $T_C = 203.5$ K reported for H_3S at $P = 155$ GPa was determined by temperature extrapolation from magnetic field sweep measurements. For the same sample, temperature dependence in zero-field-cooled magnetization and electrical resistivity indicate lower superconducting onset temperatures, 200.4 K and 195.8 K, respectively, while zero resistance

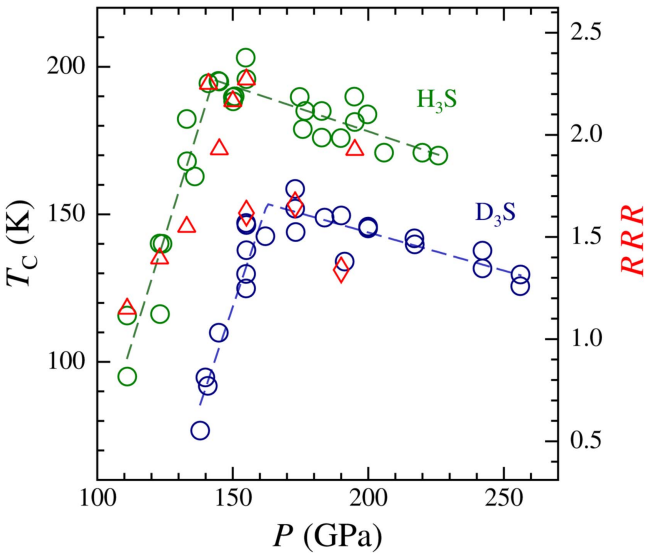

Figure 1. Transition temperatures T_C for H_3S (green circles) and D_3S (blue circles) versus applied pressure P with corresponding dashed lines fitted to joined linear trends using equation (1) with parameters in table 1 (left scale). Residual resistance ratios *RRR* are shown for H_3S (red triangles) and D_3S (red diamonds) versus P (right scale). Data are for samples annealed at or above room temperature [1, 2].

appears to set in below 170 K (as read from figure 4(a) of [1]). Field-cooled magnetization data exhibit no evidence of the superconducting transition or Meissner flux exclusion, which has been attributed to formation of fluxons strongly pinned to material defects.

Methods and results

Obtained from measurements of resistance and magnetic transitions, results for T_C indicate a maximum in the dependence on P, along with an H–D isotope dependent difference, as shown in figure 1. Data for T_C versus P are read from figure 2(c) of [1] and figure 3(c) of [2]. Additional data for figure 1 are T_C determined from superconducting onset temperatures in resistance-versus-temperature $R(T)$ traces shown in figures 2(b), 3(b), and 4(a) of [1] and figures 3(a) and (b) of [2], together with the associated values of P. As indicated in figure 3(c) of [2], the regions of highest T_C appear to distinguish R3m crystal structure at lower P and $Im\bar{3}m$ structure at higher P, although a structural distinction was not clearly discernible from these x-ray diffraction experiments.

Despite substantial scatter among the data points in figure 1, several qualitative features are clearly evident: (1) T_C for H_3S is generally higher than T_C for D_3S; (2) the region of maximum T_C for H_3S occurs at lower P than for D_3S; and (3) T_C shows pronounced linear-like variations at low P and comparatively shallow linear-like variations at high P. These characteristics can be represented by modeling T_C as a piecewise linear function of P,

$$T_C(p) = T_m[1 - a(1-p)\theta_{hv}(1-p) - b(p-1)\theta_{hv}(p-1)], \quad (1)$$

Table 1. Values of parameters T_m, P_m, a, and b from fitting equation (1) to data for T_C versus P in figure 1 for H_3S and D_3S. Statistical uncertainties in the two least significant digits are given in parentheses; fitting rms deviation is given by σ_{fit}.

	T_m (K)	P_m (GPa)	a	b	σ_{fit} (K)
H_3S	195.6(3.0)	142.9(1.9)	2.16(18)	0.224(55)	8.3
D_3S	153.5(3.0)	162.7(1.8)	2.91(26)	0.274(61)	6.6

written in terms of reduced pressure $p = P/P_m$, corresponding to a maximum temperature T_m at pressure P_m, and slopes a and b; θ_{hv} is the Heaviside unit step function. Fits of equation (1) are displayed as the dashed lines in figure 1; the fitted parameters are given in table 1; σ_{fit} is the root-mean-square deviation between the function of equation (1) and measured T_C and indicates the experimental reproducibility is 7–8 K. The fitted pressure P_m at the T_m-point for D_3S is higher, relative to H_3S, by 19.8 ± 2.6 GPa, which compares well to the 18 GPa pressure difference associated with the highest T_C measured for each isotope in figure 1.

Information contained in recordings of resistance versus temperature $R(T)$ for samples annealed at room temperature, of which eight are available for H_3S and three for D_3S [1, 2], illustrate a correlation between normal-state temperature dependence and the width of the superconducting transition. The temperature dependence is represented by the residual resistance ratio $RRR = R(T_{C0})/R(0)$, using as reference temperatures the highest measured $T_{C0} = 203.5$ K and $T = 0$, as determined from linear extrapolations of $R(T)$ in the normal-state region $T > T_C$, where $R(T)$ is nearly linear in T. As customarily applied to metals with room temperature as the upper reference point, *RRR* provides a specific measure for distinguishing relative order or purity among samples; e.g., optimal high-T_C superconductors in the clean limit generally have $RRR \gg 1$, and depression in T_C has been found to follow depression in *RRR* [9]. The data for *RRR* are shown in figure 1, scaled on the right ordinate axis. As is clearly observable, the maxima in the P dependence of T_C are clearly correspondingly correlated with maxima in *RRR*. By way of comparison, H_3S samples not annealed at room temperature display smaller $RRR \lesssim 1.06$ and are semiconductor-like for $P < P_m$ (from figure 1(a) of [1]).

The relative transition width $\Delta T_C/T_C$ provides a quantitative measure to compare homogeneity in the superconducting states of various samples. The width of the superconducting transition can be determined from the transition midpoint where $R(T_{½}) = ½\ R(T_C)$ and defined as $\Delta T_C = T_C - T_{½}$. Results from the eleven $R(T)$ measurements are shown as *RRR* versus $\Delta T_C/T_C$ in figure 2, where the dashed line is a linear fit indicating the trend among the data points. The systematic decreases in *RRR*, accompanied by systematic increases in $\Delta T_C/T_C$, show that the three D_3S samples have lesser metallic order and superconducting homogeneity, when compared to the five H_3S samples with highest order and sharpest superconducting transitions. Applied pressures for these five H_3S samples and the three D_3S samples correspond to $P \gtrsim P_m$. The data for the three

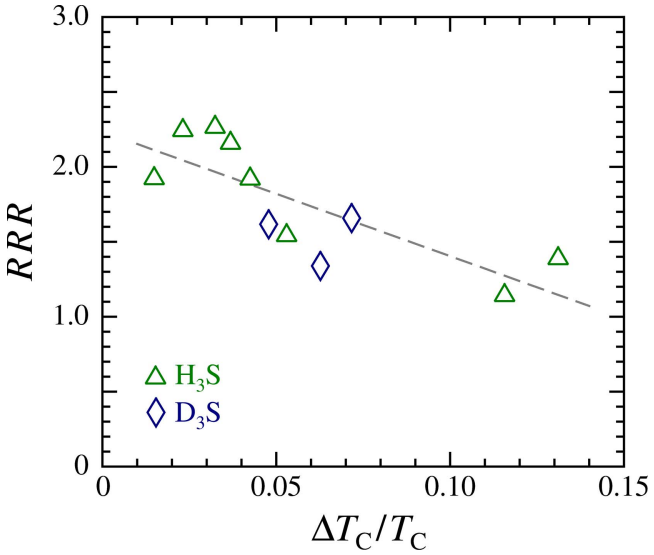

Figure 2. Residual resistance ratio *RRR* versus fractional transition width $\Delta T_C/T_C$ for samples of H_3S (green triangles) and D_3S (blue diamonds). A linearly fitted dashed line is drawn to indicate the trend.

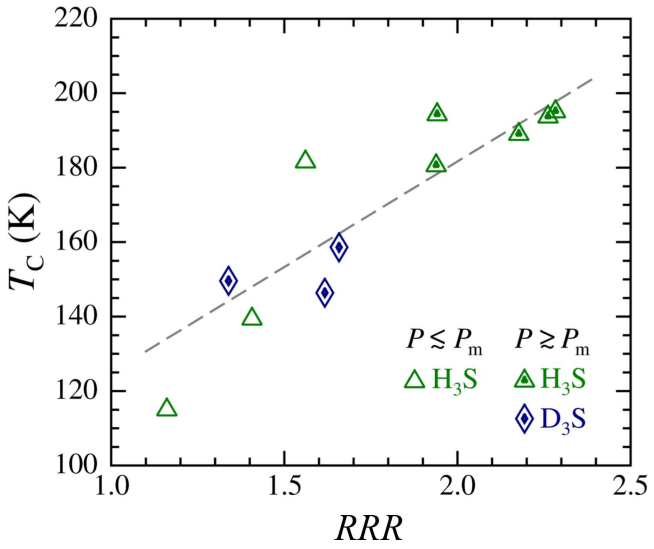

Figure 3. Transition temperature T_C versus residual resistance ratio *RRR* for H_3S (green triangles) and D_3S (blue diamonds). The eight symbols with dot fill correspond to data for $P \gtrsim P_m$ with trend shown by the fitted dashed line.

H_3S samples with relatively broad superconducting transitions ($\Delta T_C/T_C > 0.05$) were obtained at pressures $P < P_m$.

A corresponding correlation also occurs between T_C and *RRR*, as shown in figure 3. Data available at $P \gtrsim P_m$ for both isotopes are indicated by the eight dot-filled symbols and show the trend given by the fitted diagonal line. The data in both figures 2 and 3 indicate lesser quality among the D_3S samples, which undoubtedly contributes to their lower values of observed T_C, relative to H_3S.

The measurements of *RRR* provide an ideal basis for comparing observed T_C between H_3S and D_3S. Figure 1 shows that there are two measurements each for H_3S and D_3S that have high values of *RRR* and are near their respective $P \approx P_m$. The data for these four measurements are given in table 2.

Table 2. Data for applied pressure P and T_C for samples of H_3S and D_3S exhibiting highest available values of residual resistance ratio *RRR* determined for reference temperatures 203.5 and 0 K. $\Delta T_C/T_C$ is the fractional width of the superconducting transition.

	P (GPa)	T_C (K)	*RRR*	$\Delta T_C/T_C$
H_3S	141	194.4	2.261	0.0232
H_3S	155	195.8	2.283	0.0324
D_3S	155	146.6	1.617	0.0478
D_3S	173	158.6	1.658	0.0717

A linear regression fit to these data of the function,

$$T_C = t_1 + t_2\, RRR, \tag{2}$$

yields the results $t_1 = 42 \pm 15$ K, $t_2 = 67 \pm 7$ K, coefficient of determination $R^2 = 0.98$, and ± 5 K fitting error. This fit is used to determine the right ordinate scale for *RRR* in figure 1, which ranges from 0.311 to 2.623 and aligns with the 60–220 K span of the left ordinate for T_C. This display of the data points in figure 1 facilitates judging the similarities in the pressure dependences of T_C and *RRR*, noting that the correlations between *RRR* and T_C found in figure 3 extend to correlations with P.

The two middle rows of table 2 contain measurements for both isotopes at the same $P = 155$ GPa, which enables extrapolating the relationship between the values of T_C for the two isotopes to theoretically equal values of *RRR*, i.e., extrapolating to equality in sample quality. This is accomplished by scaling the transition temperatures, $T_C^{H_3S}$ and $T_C^{D_3S}$, of H_3S and D_3S, respectively:

$$T_C^{D_3S} = S\, T_C^{H_3S}. \tag{3a}$$

The scaling parameter S is determined from equation (2) and the residual resistance ratios, RRR_{H_3S} and RRR_{D_3S} for H_3S and D_3S, respectively, at matching values of P according to,

$$S = (RRR_{D_3S} + t_1/t_2)/(RRR_{H_3S} + t_1/t_2). \tag{3b}$$

With the parameters t_1 and t_2 from the fit of equation (2) and data for *RRR* at $P = 155$ GPa in table 2, one obtains the result $S = 0.770 \pm 0.108$.

A measurement of *RRR* is also available for each isotope in the region $P > P_m$ at comparable values of P (see figure 1); the data are $P = 195$ GPa, $T_C = 181.3$ K, and $RRR = 1.938$ for H_3S and $P = 190$ GPa, $T_C = 149.6$ K, and $RRR = 1.339$ for D_3S. For these two points, the formula of equation (3*b*) evaluates to $S = 0.765$. Hence, the implication is that S is a constant in the region $P \gtrsim P_m$, where T_C decreases with increasing P.

Isotope effect exponent

Having determined the scaling parameter S, the mass isotope effect exponent α may be calculated under the criterion of holding *RRR* as theoretically constant, i.e., treating H_3S and D_3S as with equivalent order (or disorder) for measurements

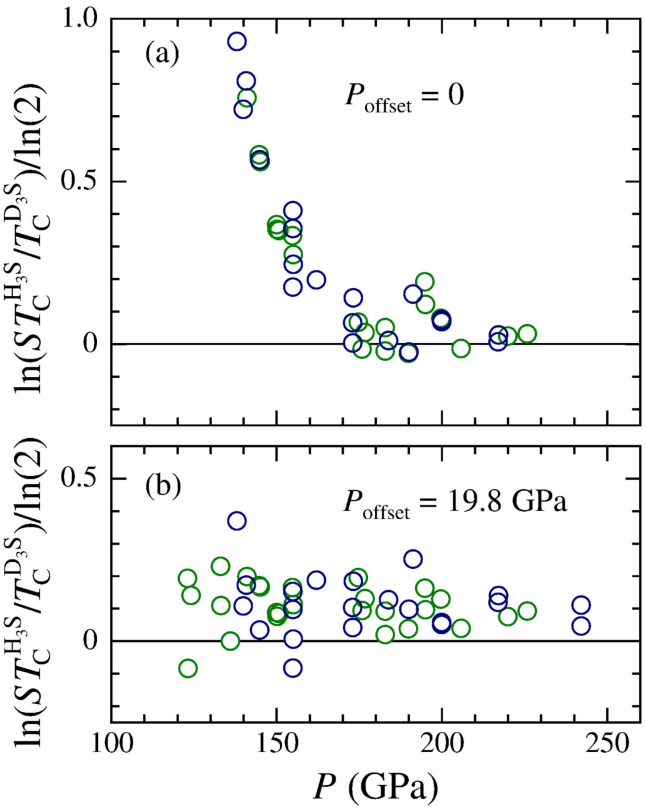

Figure 4. Mass isotope effect formula in equation (4) versus applied pressure P; frames (a) and (b) correspond to $P_{offset} = 0$ and 19.8 GPa, respectively. Green circles are from H_3S data and interpolated D_3S data; blue circles are from D_3S data and interpolated H_3S data.

of T_C at equal applied pressures. From the definition of the mass isotope exponent in T_C, the expression applied to the data is,

$$\alpha = \ln(ST_C^{H_3S}/T_C^{D_3S})/\ln(2). \quad (4)$$

For the data at $P = 155$ GPa in table 2, equation (4) evaluates to $\alpha = 0.043 \pm 0.140$. For the data at $P = 190$–195 GPa cited above, one obtains $\alpha = -0.11 \pm 0.14$.

Extension of the calculation to obtain pressure dependence with an assumed fixed $S = 0.77$ is shown in figure 4 according to two methods of treating the T_C data in figure 1. In figure 4(a), the expression of equation (4) is evaluated from the $T_C(P)$ data of a given isotope and the interpolated T_C data of the other isotope. The results cover the range 138 GPa $\leqslant P \leqslant$ 226 GPa where the data for P are overlapping. The pronounced increase in apparent α occurring at low pressure comes about because $T_C^{D_3S}$ falls off more rapidly with reduced P than does $T_C^{H_3S}$.

The correlated decreases in *RRR* and T_C shown in figures 1 and 3 for H_3S at $P < P_m$ suggests that extrinsic disorder depresses the observed T_C in such samples. Although *RRR* data for $P < P_m$ are presently available only for H_3S, the similarities shown in T_C for $P < P_m$ suggests that degradation of sample quality for both H_3S and D_3S underlies the anomalous increase in α at low pressure. In view of the isotope shift in P_m, an approach to testing this hypothesis for the region $P < P_m$ is to evaluate equation (4) with $T_C^{H_3S}$ at a given P and interpolated $T_C^{D_3S}$ at $P + P_{offset}$, and vice versa with $T_C^{D_3S}$ at a given P and interpolated $T_C^{H_3S}$ at $P - P_{offset}$. Results obtained for $P_{offset} = 19.8$ GPa based on table 1 are shown in figure 4(b), where the green and blue circles denote results for H_3S and D_3S at given P, respectively. This treatment essentially eliminates the low-P upturn in α, giving on average $\alpha = 0.13 \pm 0.11$ for $P \lesssim 160$ GPa, a result consistent with the hypothesis and a constant S, albeit presumed to be 0.77. A theoretical $\alpha = 0.25$ calculated for a low-T_C phase [7] may be compared to this result.

In the regions corresponding to $P \gtrsim P_m$ for both H_3S and D_3S, the T_C data are more weakly dependent on P (factor ~10 smaller slopes, table 1) such that the results for α are presumably less influenced by variations in disorder with P. This region corresponds to the data for $P > 160$ GPa in figure 4(a); considering that such results are derived directly from T_C data, one obtains on average $\alpha = 0.048 \pm 0.068$, where the uncertainty is the statistical standard deviation.

Conclusion

An experimentally accurate value of $\alpha = 0.043 \pm 0.140$ is derived from measurements of transition temperature T_C and residual resistance ratios *RRR* for H_3S and D_3S at applied pressure $P = 155$ GPa, which is in the region yielding maximum T_C. The value of α as defined in equation (4) depends upon the scaling parameter S, which is in turn determined from *RRR* data. The obvious inverse correlation between *RRR* and the fractional transition width $\Delta T_C/T_C$, as shown in table 2, supports identifying the former as an accurate measure of relative sample order. The aforecited theoretical predictions [4–6], about twice the uppermost limit $\alpha \leqslant 0.183$ obtained from the data, are in conflict with an experimental α for which the uncertainty also implies consistency with zero. It is evident that materials-based isotopic effects play critically important roles in determining T_C, particularly for D_3S, which have heretofore been neglected. The isotope effect in P_m and the associated depressed T_C and *RRR* for $P < P_m$ appear to reflect differing R3m–Im$\bar{3}$m transition pressures [5]. There is also an isotope effect in room temperature annealing, suggesting that a comparatively higher kinetic barrier allows for higher residual disorder in D_3S, relative to H_3S. As deduced from *RRR* data for H_3S, the apparent anomalous increase in α at low pressures is affected by degraded sample quality at low pressures. The relatively lower values of *RRR* measured for H_3S and D_3S at $P = 190$–195 GPa suggests decreased T_C at higher pressures correlates with reduced sample quality (and a degraded superconducting state) as well. Other observations corroborating issues with materials quality are 7–8 K reproducibilities in T_C measurements, differences between resistance and magnetic measurements of T_C, depressed zero-resistance temperatures, and the absence of field-cooled flux exclusion below T_C.

Acknowledgments

The authors are grateful for support from the College of William and Mary, the New Jersey Institute of Technology, and the University of Notre Dame.

References

[1] Drozdov A P, Eremets M I, Troyan I A, Ksenofontov V and Shylin S I 2015 Conventional superconductivity at 203 K at high pressures in the sulfur hydride system *Nat. Lett.* **525** 73–84

[2] Einaga M, Sakata M, Ishikawa T, Shimizu K, Eremets M I, Drozdov A P, Troyan I A, Hirao N and Ohishi Y 2016 Crystal structure of the superconducting phase of sulfur hydride *Nat. Phys.* **12** 835–9

[3] Duan D, Liu Y, Tian F, Li D, Huang X, Zhao Z, Yu H, Liu B, Tian W and Cui T 2014 Pressure-induced metallization of dense $(H_2S)_2H_2$ with high-T_c superconductivity *Sci. Rep.* **4** 6968

[4] Errea I, Calandra M, Pickard C J, Nelson J, Needs R J, Li Y, Liu H, Zhang Y, Ma Y and Mauri F 2015 High-pressure hydrogen sulfide from first principles: a strongly anharmonic phonon-mediated superconductor *Phys. Rev. Lett.* **114** 157004

[5] Errea I, Calandra M, Pickard C J, Nelson J R, Needs R J, Li Y, Liu H, Zhang Y, Ma Y and Mauri F 2016 Quantum hydrogen-bond symmetrization in the superconducting hydrogen sulfide system *Nature* **532** 81–95

[6] Akashi R, Kawamura M, Tsuneyuki T, Nomura Y and Arita R 2015 First-principles study of the pressure and crystal-structure dependences of the superconducting transition temperature in compressed sulfur hydrides *Phys. Rev.* B **91** 224513

[7] Gor'kov L P and Kresin V Z 2016 Pressure and high-T_c superconductivity in sulfur hydrides *Sci. Rep.* **6** 25608

[8] Jarlborg T and Bianconi A 2016 Breakdown of the Migdal approximation at Lifshitz transitions with giant zero-point motion in the H_3S superconductor *Sci. Rep.* **6** 24816

[9] Harshman D R and Fiory A T 2012 Charge compensation and optimal stoichiometry in superconducting $(Ca_xLa_{1-x})(Ba_{1.75-x}La_{0.25+x})Cu_3O_y$ *Phys. Rev.* B **86** 144533